

## Time Variation of Effective Climate Sensitivity in GCMs

K. D. WILLIAMS

*Met Office Hadley Centre, Exeter, United Kingdom*

W. J. INGRAM

*Met Office Hadley Centre, Exeter, and Department of Physics, University of Oxford, Oxford, United Kingdom*

J. M. GREGORY

*Met Office Hadley Centre, Exeter, and Walker Institute for Climate System Research, Department of Meteorology, University of Reading, Reading, United Kingdom*

(Manuscript received 6 December 2007, in final form 28 February 2008)

### ABSTRACT

Effective climate sensitivity is often assumed to be constant (if uncertain), but some previous studies of general circulation model (GCM) simulations have found it varying as the simulation progresses. This complicates the fitting of simple models to such simulations, as well as having implications for the estimation of climate sensitivity from observations. This study examines the evolution of the feedbacks determining the climate sensitivity in GCMs submitted to the Coupled Model Intercomparison Project. Apparent centennial-time-scale variations of effective climate sensitivity during stabilization to a forcing can be considered an artifact of using conventional forcings, which only allow for instantaneous effects and stratospheric adjustment. If the forcing is adjusted for processes occurring on time scales that are short compared to the climate stabilization time scale, then there is little centennial-time-scale evolution of effective climate sensitivity in any of the GCMs. Here it is suggested that much of the apparent variation in effective climate sensitivity identified in previous studies is actually due to the comparatively fast forcing adjustment.

Persistent differences are found in the strength of the feedbacks between the coupled atmosphere–ocean (AO) versions and their atmosphere–mixed layer ocean (AML) counterparts (the latter are often assumed to give the equilibrium climate sensitivity of the AOGCM). The AML model can typically only estimate the equilibrium climate sensitivity of the parallel AO version to within about 0.5 K. The adjustment to the forcing to account for comparatively fast processes varies in magnitude and sign between GCMs, as well as differing between AO and AML versions of the same model. There is evidence from one AOGCM that the forcing adjustment may take a couple of decades, with implications for observationally based estimates of equilibrium climate sensitivity. It is suggested that at least some of the spread in twenty-first-century global temperature predictions between GCMs is due to differing adjustment processes, hence work to understand these differences should be a priority.

### 1. Introduction

Equilibrium climate sensitivity, defined as the equilibrium global-mean temperature response to doubling CO<sub>2</sub> ( $T'_{eq}$ ), is a leading-order measure of the response of the climate system to an external forcing. It is widely used in comparing the response of different general circulation models (GCMs) employed for anthropo-

genic climate change projections (e.g., Randall et al. 2007; Murphy et al. 2004; Stainforth et al. 2005). Running a full coupled atmosphere–ocean (AO) GCM to equilibrium can require several millennia of model simulation and this computational expense is prohibitive in general. Instead, the equilibrium climate sensitivity of a GCM is usually estimated from coupling its atmosphere component to a thermodynamic mixed layer ocean model (AML). AML models typically achieve equilibrium within a few decades and so are computationally more affordable. It is often assumed that  $T'_{eq}$  obtained from an AML model will equal  $T'_{eq}$

---

*Corresponding author address:* Keith Williams, Met Office Hadley Centre, FitzRoy Road, Exeter, EX1 3PB, United Kingdom.  
E-mail: keith.williams@metoffice.gov.uk

from the parallel AO model if it were run to equilibrium. But, the effects of dynamic ocean processes (e.g., slowing of the thermohaline circulation) and different control climates on atmospheric processes (e.g., cloud response) make this assumption only approximate. Boer and Yu (2003c) find that for a previous version of the Canadian Centre for Climate Modelling and Analysis (CCCma) model, the feedbacks in the AO model near equilibrium differ from the AML model due to a mean El Niño-like pattern developing in the AO model, altering the cloud feedback. In contrast, Williams et al. (2001b) find that for a previous version of the Met Office Hadley Centre model (HadCM2) (Johns et al. 1997), which also produces a mean El Niño-like pattern, the feedbacks in the AO model and AML model are qualitatively similar since the El Niño-like pattern also develops in the AML model (i.e., it is driven by atmospheric rather than ocean processes in that case).

An alternative measure of the response of the climate system that may be applied to AO model simulations without running to equilibrium is the effective climate sensitivity ( $T'_{\text{eff}}$ ) (Murphy 1995). Here  $T'_{\text{eff}}$  is an estimate of  $T'_{\text{eq}}$  for an AO model assuming that the external forcing and the feedback processes would remain constant as the system continues toward equilibrium. If we believe  $T'_{\text{eff}}$  is constant in the real world, the global warming observed so far, or models that describe it well, could be used as a quantitative guide to the future. But, if we believe it may well be variable in the real world, it may be much more difficult to constrain future warming.

Senior and Mitchell (2000, hereafter SM00) find that for HadCM2, when the forcing of the AO model is fixed at  $2 \times \text{CO}_2$  and run toward equilibrium, the total clear-sky feedback remains reasonably constant while the cloud feedback varies. This is attributed to changes in the lapse rate, caused by the slower thermal response of the Southern Ocean relative to the atmosphere, affecting the convective cloud response. They indicate that this results in  $T'_{\text{eff}}$  increasing as the HadCM2 simulation approaches equilibrium. Kiehl et al. (2006) also find  $T'_{\text{eq}}$  to be higher than the  $T'_{\text{eff}}$  calculated for the initial time of  $\text{CO}_2$  doubling for different versions of the National Center for Atmospheric Research (NCAR) model. Boer and Yu (2003a) show the opposite variation, with  $T'_{\text{eff}}$  reducing in the CCCma model as the climate warms owing to a strengthening (more negative) shortwave cloud feedback, although the clear-sky feedbacks also show more dependence on climate state in this model than reported by SM00 for HadCM2.

Previous studies investigating time/state variation of effective climate sensitivity have used the conventional

stratosphere-adjusted forcing ( $f_{\text{strat}}$ ) in the calculation of climate sensitivity (although methods used have varied in detail). This approach includes the rapid radiative adjustment of the stratosphere within the “forcing” but does not permit any response from the troposphere. An alternative approach is to also allow for adjustment processes in other parts of the climate system that act on shorter time scales than the response being considered (Hansen et al. 2002; Shine et al. 2003; Gregory et al. 2004). Historically, these have mainly been associated with the indirect effects of aerosols (e.g., Williams et al. 2001a), but recently have been shown to occur with changes in  $\text{CO}_2$  (Gregory and Webb 2008, hereafter GW08; Lambert and Faull 2007; Andrews and Forster 2008).

In this study, we examine the evolution of the feedbacks during stabilization at  $2 \times \text{CO}_2$  in models submitted to the World Climate Research Programme Coupled Model Intercomparison Project phase 3 (WCRP CMIP3) multimodel dataset (also known as the IPCC Fourth Assessment Report database). We consider the extent to which the feedbacks vary with time and climate state and how this depends on the definition of “forcing,” as well as the extent to which the strength of the global feedback differs between the AO and AML models. The models and experimental design are introduced in the next section. The time variation of effective climate sensitivity in the CMIP3 models is investigated in section 3, and the AO and AML feedbacks are compared in section 4. Mechanisms to account for the differences between the different types of forcing are presented in section 5. Conclusions and discussion are in section 6.

## 2. Models and experimental design

The models used in this study and references to their descriptions are listed in Table 1. Parallel control and climate change simulations have been performed with each AO model. The control maintains fixed concentrations of  $\text{CO}_2$  and other natural and anthropogenic forcing agents [generally these are preindustrial values, but the Community Climate System Model, version 3 (CCSM3) uses present-day values]. Averages over the whole control simulation are used, which is a period of at least 100 yr in each case. Control drift does not significantly impact the results presented here. The climate change simulation has  $\text{CO}_2$  concentration increased at  $1\% \text{ yr}^{-1}$  for 70 years, by which time the  $\text{CO}_2$  concentration has reached double the control value. The  $\text{CO}_2$  concentration is then held constant at double the control levels and the simulation continued for at least a further 150 yr. In the case of HadCM3 and the

TABLE 1. List of CMIP3 models used in this study. Although the full model name is listed in this table, shortened names will be used elsewhere in the paper. Horizontal resolution is prefixed by “T” for the triangular truncation of spectral models and “N” for half the number of east–west points for gridpoint models (giving approximately comparable numbers). The number of atmosphere levels is prefixed by “L.”

Model	Atmospheric resolution	Main references
CCSM3	T85 L26	Collins et al. (2006)
CGCM3.1(T47)	T47 L31	<a href="http://www.cccma.bc.ec.gc.ca/models/cgcm3.shtml">http://www.cccma.bc.ec.gc.ca/models/cgcm3.shtml</a>
ECHAM5/Max Planck Institute Ocean Model (MPI-OM)	T63 L31	Roeckner et al. (2003)
GFDL-Climate Model version 2.0 (CM2.0)	N72 L24	Delworth et al. (2006)
GISS-Model E-R (ER)	N45 L20	Schmidt et al. (2006)
Model for Interdisciplinary Research on Climate 3.2, medium-resolution version [MIROC3.2(medres)]	T42 L20	K-1 Model Developers (2004)
Met Office Unified Model (MetUM)-HadCM3	N48 L19	Pope et al. (2000); Gordon et al. (2000)
MetUM-HadGEM1	N96 L38	Martin et al. (2006); Johns et al. (2006)

Hadley Centre Global Environmental Model version 1 (HadGEM1), we have access to 500 years of stabilization data (the period during which CO<sub>2</sub> is held fixed from the initial time of CO<sub>2</sub> doubling) that is not currently in the CMIP3 database.

The AML version of each model uses the same atmospheric component as the AO model, but coupled to a simple thermodynamic mixed layer ocean model. The AML models have been run to equilibrium with both preindustrial and twice preindustrial CO<sub>2</sub> concentrations, and we use averages over 20 yr once equilibrium is achieved.

We examine all the models in the CMIP3 database that have both AO and parallel AML experiments available and, for the AO climate change experiment, more than 150 yr of stabilization after CO<sub>2</sub> concentrations are doubled.

The stratospherically adjusted  $2 \times$  CO<sub>2</sub> forcing diagnosed at the tropopause was obtained from the CMIP3 database for each model. For most of the GCMs, shortwave and longwave, clear-sky and all-sky components of the forcing are available. The difference between the all-sky and clear-sky is used to give the cloud components of the stratosphere-adjusted forcing. For CCCma Coupled General Circulation Model, version 3.1 (CGCM3.1) and Geophysical Fluid Dynamics Laboratory (GFDL) models only all-sky shortwave and longwave components are available, so the cloud component is assumed to be zero when decomposed stratosphere-adjusted forcings are used below.

### 3. Evolution of effective climate sensitivity in the CMIP3 models

The notation used in this paper follows Boer and Yu (2003b). The signed feedback parameter ( $\Lambda$ ) is given by

$$\Lambda = \frac{(R' - f)}{T'}, \quad (1)$$

where  $f$  is the forcing imposed on the climate system,  $R'$  is the radiative imbalance (positive downward) at the top of the atmosphere (TOA), and  $T'$  is the transient global-mean surface temperature response. Thus a positive feedback (one that tends to increase  $T'$ ) will make  $\Lambda$  more positive/less negative, and vice versa. Here  $\Lambda$  must be negative if the system is to be stable and reach a new equilibrium in the presence of the forcing. The effective climate sensitivity ( $T'_{\text{eff}}$ ) (Murphy 1995) is then calculated as

$$T'_{\text{eff}} = -\frac{f}{\Lambda} = -\frac{1}{(R'/f) - 1} T'. \quad (2)$$

As noted in the introduction, there are different methods available for calculating the forcing. The conventional approach is to calculate the instantaneous radiative perturbation but allowing for the rapid adjustment of the stratosphere ( $f_{\text{strat}}$ ) (e.g., Houghton et al. 2001). This method has been used by previous studies investigating time/state dependence of effective climate sensitivity (e.g., SM00; Boer and Yu 2003a). However, GW08 show that fast response processes in the troposphere that occur before the surface temperature responds can have a significant effect on  $R'$ . Fixed (sea) surface temperature experiments have been proposed by Hansen et al. (2002) and Shine et al. (2003) to calculate this “troposphere-adjusted forcing.” A third approach, proposed by Gregory et al. (2004), is to plot  $R'$  against  $T'$ . If the effective climate sensitivity remains constant for the period being considered, then the data points will lie on a straight line with gradient  $\Lambda$  [from Eq. (1)]. Regression of the straight line to intercept with the  $R'$  axis will give an “effective forcing,” which is

adjusted for processes happening on shorter time scales than the first data point lying close to the regression line. For example, if annual means are plotted for an AML model starting from an instantaneous doubling of  $\text{CO}_2$  and all the data points are on a straight line, then the intercept will be an effective forcing adjusted for fast processes that have been completed on time scales less than 1 yr. We will denote this  $f_{\text{eff}}$  to indicate the effective forcing that has been adjusted for all processes acting on time scales that are short compared with the stabilization period. This forcing adjustment will include stratospheric and tropospheric adjustment; it may also include other relatively fast processes in the climate system such as rapid warming of the land surface.

The regression of  $R'$  against  $T'$  has been performed on decadal-mean stabilization data for the AO models. The intercept with the  $R'$  axis provides  $f_{\text{eff}}$  (which includes “fast” processes operating during the 70-yr 1%  $\text{yr}^{-1}$  ramp to  $2 \times \text{CO}_2$ ). The solid line in Fig. 1a shows an example of this regression for HadCM3. By regressing clear-sky atmosphere, cloud, shortwave, and longwave components of  $R'$  separately, the components of  $f_{\text{eff}}$  and  $\Lambda$  may be calculated. Following Boer and Yu (2003b), these are denoted with subscripts A (clear-sky atmosphere), C (cloud), S (shortwave), and L (longwave); for example, subscript SA indicates clear-sky shortwave. The cloud components are calculated as a difference between the all- and clear-sky components (e.g., Cess et al. 1990). This convenient approach has been widely used, but it should be borne in mind that cloud masking of water vapor and sea/land ice means a change in this measure of the cloud component is possible without a change in cloud (e.g., Zhang et al. 1994; Soden et al. 2004, 2008). Since separate regressions are calculated for  $\Lambda$  and its components, the total  $f_{\text{eff}}$  does not exactly equal the sum of the  $f_{\text{eff}}$  components (GW08), although the differences are small in practice. Similar regressions have been calculated from annual mean data for the parallel AML models in which  $\text{CO}_2$  was instantaneously doubled (these have previously been documented by GW08). For some of the GCMs,  $f_{\text{eff}}$  is statistically significantly different between the AO and AML models (an issue that we will address further in section 5); hence we use each model version’s own  $f_{\text{eff}}$  in the subsequent analysis of the AO and AML versions. Exceptions to this are CGCM3.1 and the Goddard Institute for Space Studies (GISS) for which the error range on  $f_{\text{eff}}$  from the AO regression is greater than  $0.5 \text{ W m}^{-2}$  for one of the components and encompasses the AML  $f_{\text{eff}}$  for all components, so for these two GCMs the AML  $f_{\text{eff}}$  is used for the AO model (the AML regression has smaller error estimates since the first data points are closer to the  $R'$  axis, but may be less

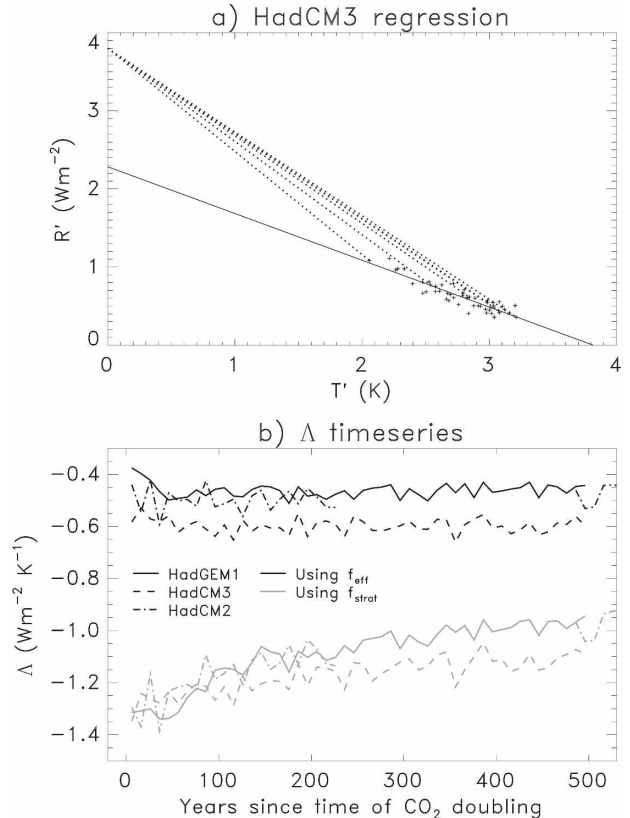


FIG. 1. (a) Decadal-mean data for the HadCM3 stabilization at  $2 \times \text{CO}_2$  following a  $1\% \text{ yr}^{-1}$   $\text{CO}_2$  ramped increase. The solid line shows a linear regression through the data. The dotted lines link the stratospherically adjusted forcing  $f_{\text{strat}}$  to every tenth data point. (b) Time series of the signed feedback parameter ( $\Lambda$ ) during the HadGEM1, HadCM3, and HadCM2 AO model stabilization at  $2 \times \text{CO}_2$ . Gray lines use  $f_{\text{strat}}$ . Black lines use the forcing calculated by the regression method ( $f_{\text{eff}}$ ). The time series have been constructed from decadal means. The HadCM2 data between years 230 and 480 have been corrupted since the analysis of SM00.

appropriate if the dynamical ocean is involved with the forcing adjustment). The  $f_{\text{strat}}$ ,  $f_{\text{eff}}$ , and effective climate sensitivities they imply at the time of  $\text{CO}_2$  doubling, together with the equilibrium climate sensitivity from the AML model, are given in Table 2. As shown by GW08, inclusion of nonstratospheric fast processes can result in a considerable change in the adjusted forcing, and consequently in  $T'_{\text{eff}}$ . However, neither forcing diagnosis results in  $T'_{\text{eff}}$  from the AO models being generally close to the AML  $T'_{\text{eq}}$  (the root-mean-square difference between  $T'_{\text{eq}}$  and  $T'_{\text{eff}}$  is 0.7 K when using  $f_{\text{strat}}$  and 0.5 K when using the best estimate of  $f_{\text{eff}}$ ).

The importance of the choice of forcing for analyzing the evolution of effective climate sensitivity is illustrated in Fig. 1a. The linear regression indicated by the solid line provides a good fit to the HadCM3 stabiliza-

TABLE 2. Forcing due to doubling CO<sub>2</sub> ( $f$ ) and effective climate sensitivity at the initial time of CO<sub>2</sub> doubling ( $T'_{\text{eff}}$ ). Results are given for the stratosphere-adjusted forcing as submitted to CMIP3, and using the regression method to include adjustment from other processes. Also shown is the equilibrium climate sensitivity ( $T'_{\text{eq}}$ ) from the AML model. The adjusted forcing for CGCM3.1 and GISS are from the AML model owing to the large uncertainty on the AO regressions. Uncertainties are  $\pm 1$  standard error from the regression. Autocorrelation has not been accounted for in these uncertainty estimates.

Model	$f_{\text{strat}}$ (W m <sup>-2</sup> )	$T'_{\text{eff}}$ using $f_{\text{strat}}$ (K)	$f_{\text{eff}}$ (W m <sup>-2</sup> )	$T'_{\text{eff}}$ using $f_{\text{eff}}$ (K)	AML $T'_{\text{eq}}$ (K)
CCSM3	4.0	2.1	2.9 $\pm$ 0.4	2.4 $\pm$ 0.5	2.7
CGCM3.1	3.3	3.0	4.0 $\pm$ 0.4	2.8 $\pm$ 0.4	3.4
ECHAM5	4.0	3.3	3.2 $\pm$ 0.3	3.7 $\pm$ 0.3	3.4
GFDL	3.5	2.1	1.7 $\pm$ 0.2	3.2 $\pm$ 0.2	2.9
GISS	4.1	2.3	3.8 $\pm$ 0.3	2.4 $\pm$ 0.3	2.7
MIROC3.2	3.1	4.4	3.2 $\pm$ 0.2	4.3 $\pm$ 0.3	4.0
HadCM3	3.8	3.0	2.3 $\pm$ 0.1	3.8 $\pm$ 0.2	3.3
HadGEM1	3.8	2.9	2.0 $\pm$ 0.1	3.4 $\pm$ 0.2	4.4

tion data and suggests little change in  $\Lambda$  during the data period. However, regression gives  $f_{\text{eff}} = 2.3 \text{ W m}^{-2}$ , which is much less than  $f_{\text{strat}} = 3.8 \text{ W m}^{-2}$ . If  $f_{\text{strat}}$  were used in the calculation of  $\Lambda$  at each data point, then  $\Lambda$  would be given by the slope of the dotted lines (drawn for every 10 data points in the figure), which can be seen to vary with  $T'$ . The result is an apparent time variation of  $\Lambda$  acting on centennial time scales (Fig. 1b), whereas there is actually a rapid forcing adjustment (largely within the ramped increase period) followed by the feedback strength remaining roughly constant. This can also be seen through Eq. (1): if the true forcing is  $f$ , then  $R' = \Lambda T' + f$ . If an incorrect forcing ( $f_{\text{wrong}}$ ) is used for  $f$  in the diagnosis of  $\Lambda$ , Eq. (1) will give  $\Lambda_{\text{wrong}} = (\Lambda T' + f - f_{\text{wrong}})/T' = \Lambda + (f - f_{\text{wrong}})/T'$ , which implies a spurious time dependence in  $\Lambda$  as  $T'$  changes and asymptotes to the wrong value, as shown by Fig. 1b.

While this illustration is for the Met Office Hadley Centre GCMs (for which we have more stabilization data), the result is generally applicable to the CMIP3 models. Table 3 shows the multimodel mean magnitude of the  $\Lambda$  time series gradient (and the  $\Lambda$  components) during the first 100 yr of stabilization. For most of the components of  $\Lambda$ , the time variation is at least twice as large when  $f_{\text{strat}}$  is used rather than  $f_{\text{eff}}$ . To some extent this may be expected since the regression derivation of  $f_{\text{eff}}$  [which minimizes  $(f - R' - \Lambda T')^2$  in the mean] differs from the adjustment to  $f$  that would minimize the variance of  $\Lambda$  {minimize  $[(f - R')/T' - \Lambda]^2$  in the mean} only in the factor of  $T'$ , which is always positive and does not vary greatly in magnitude (Fig. 2a), so using  $f_{\text{eff}}$  tends to flatten  $\Lambda$  on average by construction.

TABLE 3. Multimodel average magnitude of the gradient of  $\Lambda$  and its components ( $\text{W m}^{-2} \text{ K}^{-1} \text{ century}^{-1}$ ) among the CMIP3 AO models, calculated through regression of decadal means during the first 100 yr of stabilization. Results are shown using  $f_{\text{strat}}$  and the best estimate of  $f_{\text{eff}}$  in the calculation of  $\Lambda$ . Uncertainties are root-mean-square  $\pm 1$  standard errors from each of the regressions.

	Using $f_{\text{strat}}$	Using $f_{\text{eff}}$
$ \overline{d\Lambda/dt} $	0.132 $\pm$ 0.015	0.041 $\pm$ 0.011
$ \overline{d\Lambda_A/dt} $	0.063 $\pm$ 0.010	0.032 $\pm$ 0.009
$ \overline{d\Lambda_C/dt} $	0.078 $\pm$ 0.014	0.029 $\pm$ 0.012
$ \overline{d\Lambda_{SA}/dt} $	0.028 $\pm$ 0.007	0.012 $\pm$ 0.007
$ \overline{d\Lambda_{SC}/dt} $	0.046 $\pm$ 0.015	0.034 $\pm$ 0.015
$ \overline{d\Lambda_{LA}/dt} $	0.069 $\pm$ 0.005	0.021 $\pm$ 0.004
$ \overline{d\Lambda_{LC}/dt} $	0.093 $\pm$ 0.007	0.031 $\pm$ 0.007

Nevertheless, if there were a substantial genuine time variation it would leave the time series of  $\Lambda$  with a strongly bowed shape. Figures 2b–h indicate that this is not the case for any of the CMIP3 models. The small variations that can be seen (e.g., for GFDL in  $\Lambda$  and GISS in  $\Lambda_{\text{LC}}$ ) are not significant; that is, the components of  $f_{\text{eff}}$  are consistent within their uncertainties with a zero gradient. We have also reanalyzed the HadCM2 data used by SM00 and find that using  $f_{\text{eff}}$  again leads to no significant change in  $\Lambda$  during the stabilization period (Fig. 1b). Therefore, it appears that there is little evolution of effective climate sensitivity in GCMs on centennial time scales, and we suggest that time/state dependence on this time scale indicated in previous studies may be an artifact of using  $f_{\text{strat}}$ .

#### 4. Comparison of the AO and AML feedbacks

In general, the AO and AML values of  $\Lambda$  can be seen to be quite different in Fig. 2, implying that the radiative response is affected by the simplification of the physics in the AML models (Boer and Yu 2003c). This largely accounts for  $T'_{\text{eff}} \neq T'_{\text{eq}}$  in Table 2, although differences in  $f_{\text{eff}}$  between the AO and AML versions of some GCMs also contribute. Fitting an exponential curve to the AO data suggests that for most of the GCMs, barring any millennial time-scale evolution of  $\Lambda$  (for instance associated with temperature thresholds that have not been reached by the AO models), the AO will not converge to the AML values at equilibrium.

Differences between the AO and AML  $\Lambda$  occur in both cloudy and clear sky responses. They might arise from differences in the long time-scale response (as proposed by Boer and Yu 2003c) and/or result from different fast adjustment processes in the two model versions producing differing adjusted climates (this is

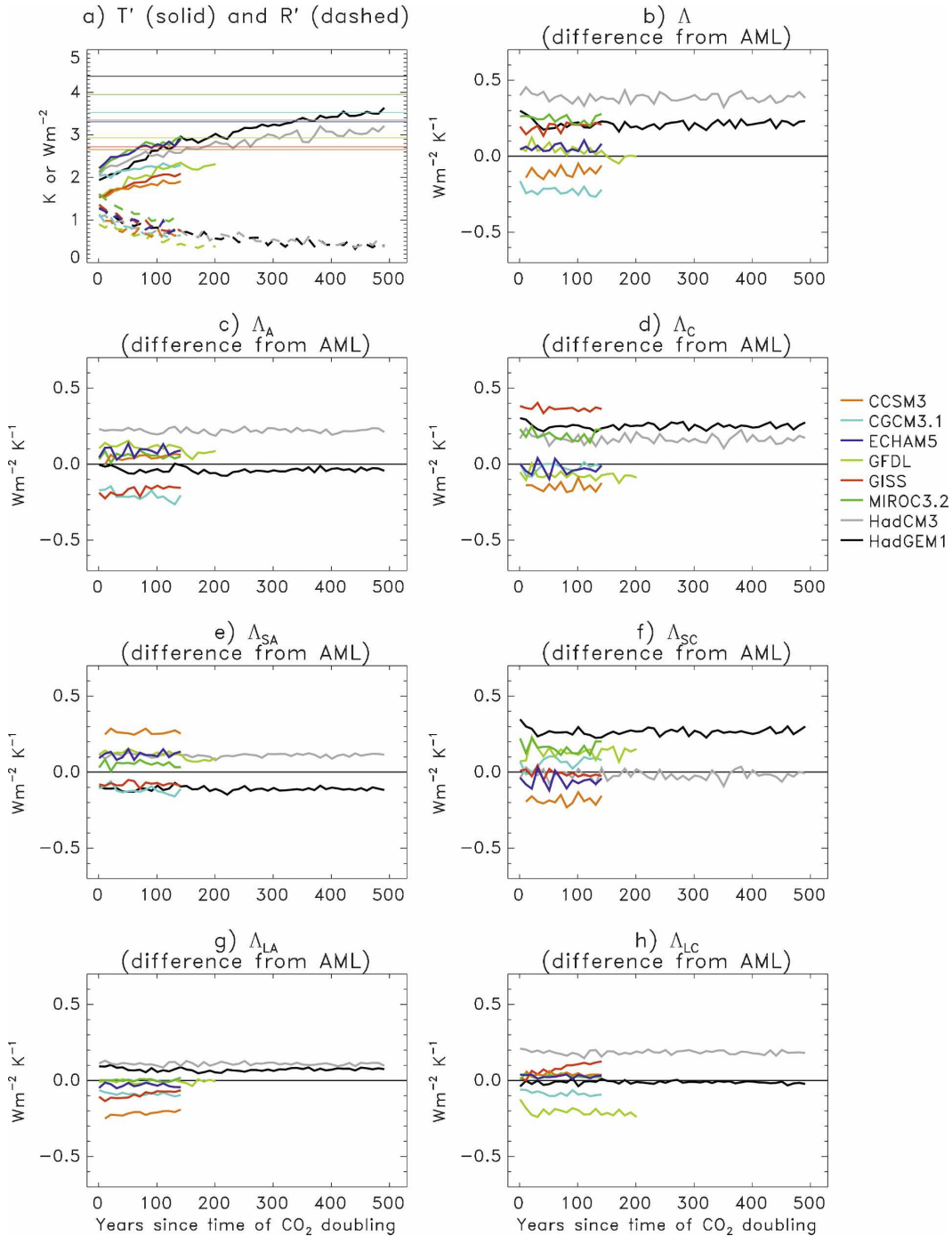


FIG. 2. Time series during the AO model stabilization at  $2 \times \text{CO}_2$  for the CMIP3 models. (a) Temperature response ( $T'$ : thick solid) and TOA imbalance ( $R'$ : dashed);  $T'_{\text{eq}}$  from the AML models are shown by the thin horizontal lines. (b)–(h) Difference of the signed feedback parameter ( $\Lambda$ ) and its components from the respective AML model (i.e.,  $\Lambda_{\text{AO}}$  minus  $\Lambda_{\text{AML}}$ ). The time series have been constructed from decadal averages.

investigated in the next section). An example of the cloud differences in the AO and AML versions of HadCM3 is shown in Fig. 3 and will include contributions from both the forcing adjustment and longer time-

scale response. Although as a first approximation, the responses of the AO and AML models are similar, the inclusion of a dynamic ocean in HadCM3 causes an increase and concentration of deep convective cloud in

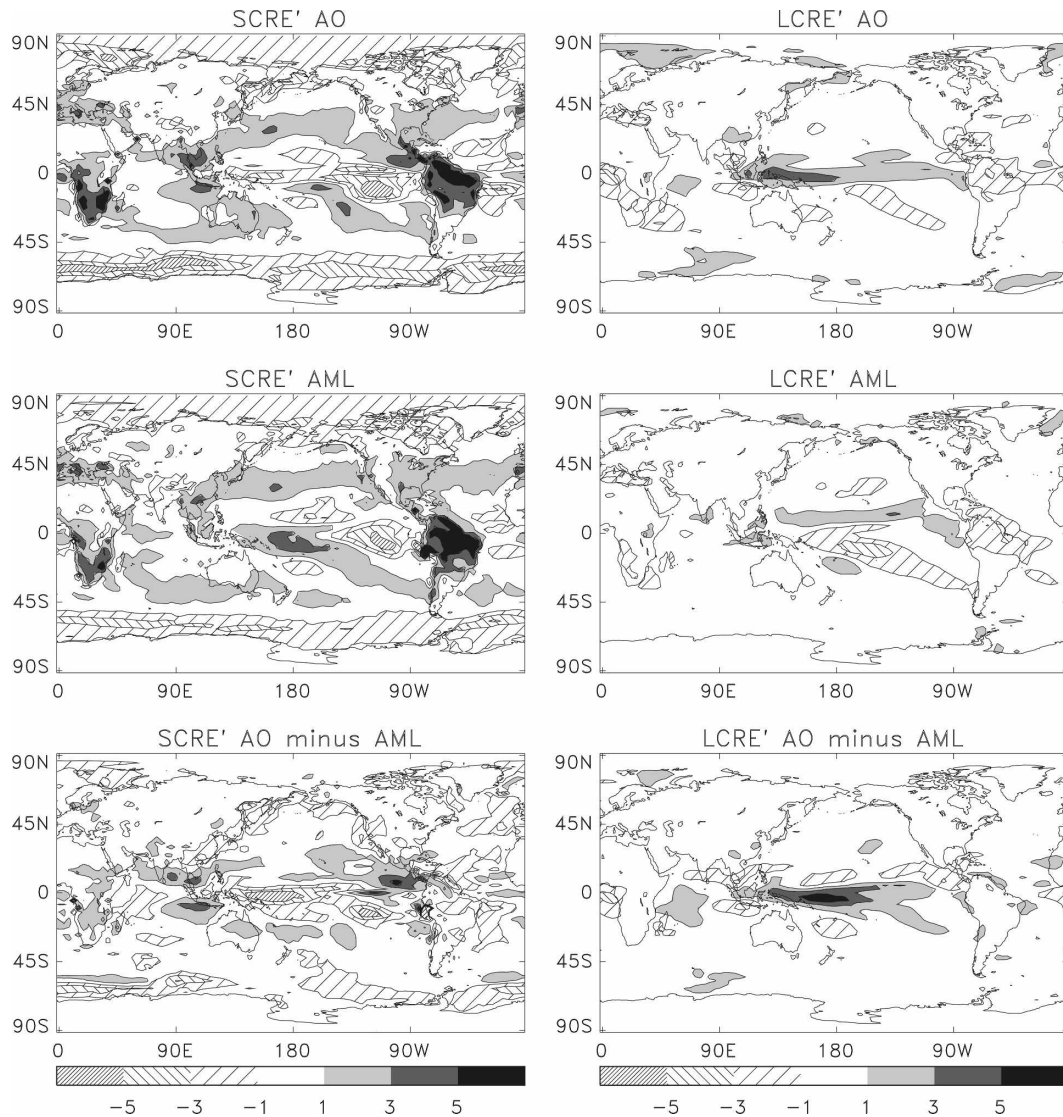


FIG. 3. HadCM3: Change in shortwave (SCRE) and longwave (LCRE) radiative effect, normalized by the global-mean surface temperature response ( $\text{W m}^{-2} \text{K}^{-1}$ ). (top) AO model after 500 yr of stabilization (mean of the final 20 yr of the simulation); (middle) AML model at equilibrium; (bottom) difference between the AO and AML models.

the tropical western Pacific, resulting in a strengthening of shortwave (negative change) and longwave (positive change) cloud radiative effect (CRE) (e.g., Cess et al. 1990) that is not present in the AML version. This is similar to the mechanism proposed by Boer and Yu (2003c), although in their AOGCM there is a mean El Niño-like response resulting in differences between the AO and AML versions over the central and eastern tropical Pacific. There are also differences in the shortwave CRE (SCRE) response due to more low cloud in the AO model over parts of the Atlantic and Southern Ocean.

The variation in  $\Lambda_{\text{SA}}$  is likely to be dominated by the

albedo feedback from melting sea ice and snow. As with the cloud components, in some of the GCMs (including HadCM3)  $\Lambda_{\text{SA}}$  is stronger in the AO simulation than in its AML counterpart, while in others (including HadGEM1) it is weaker (Fig. 2). HadGEM1 AML simulates more sea ice over the Southern Ocean in the preindustrial control than HadGEM1 AO, resulting in more ice being available to melt in the climate change experiment, while HadCM3 AML simulates less sea ice there than HadCM3 AO. This highlights the importance of ocean processes on the ice coverage in the control simulation. In these two GCMs, the same sea ice model is used in the AO and AML versions, but

some groups have simplified the scheme in the AML model (e.g., Kiehl et al. 2006). Consequently it cannot be expected that the feedbacks will be the same in the two versions and implies that AML models may be inappropriate for analyzing the corresponding AO model's sea ice feedback. The cause of the differences in  $\Lambda_{LA}$  between the AO and AML models is unclear. It is possible that changes in ocean circulation in the AO model and/or differences in other feedbacks (cloud and sea ice) result in a different latitudinal distribution of the warming between the two versions, which affects the magnitude of the global-mean water vapor feedback.

## 5. Mechanisms behind differences between $f_{\text{eff}}$ and $f_{\text{strat}}$

### a. Components of the forcing adjustment

The difference between  $f_{\text{eff}}$  and  $f_{\text{strat}}$  represents changes to  $R'$  occurring from adjustment processes (other than those in the stratosphere) that operate on time scales that are rapid compared with those of global climate change. We will simply refer to this as "forcing adjustment." The forcing adjustment, together with its radiative components, is shown for each GCM in Fig. 4. There is little agreement in the magnitude or sign of this forcing adjustment, either in the net or in the individual components. Consequently, the forcing adjustment processes represent a significant contribution to the overall uncertainty in the response to an external forcing (also noted by GW08; Lambert and Faull 2007). The Met Office Hadley Centre models have among the largest net forcing adjustments, and we analyze the mechanisms responsible in these GCMs here. However, further research is required to understand why the forcing adjustment processes vary to such an extent between the CMIP3 models.

In both HadGEM1 and HadCM3, the largest component to the forcing adjustment is in the clear-sky longwave. An important caveat on the results in Fig. 4 is that  $f_{\text{strat}}$  has been calculated at the tropopause while  $f_{\text{eff}}$  is at the TOA. It is possible that some of the clear-sky longwave and shortwave forcing adjustment is associated with the different level of diagnosis, but the longwave and shortwave components of such an artifact should largely cancel (Gregory et al. 2004). Since the forcing adjustment in LA is much larger than SA in HadGEM1 and HadCM3, we believe that most of the LA adjustment is a real response of the modeled climate system. The negative LA forcing adjustment is largest in both GCMs in the Northern Hemisphere and tropics (Fig. 5). It is also larger over land than sea ( $-1.32 \text{ W m}^{-2}$  versus  $-0.75 \text{ W m}^{-2}$  in HadCM3 and

$-1.94 \text{ W m}^{-2}$  versus  $-0.87 \text{ W m}^{-2}$  in HadGEM1 for land versus sea, respectively). Extrapolation of the regressed change in specific humidity change against change in surface temperature to zero temperature change reveals little evidence for a rapid response of water vapor in these models. We therefore suggest that most of the LA forcing adjustment in the Met Office Hadley Centre models is due to a rapid warming of the land surface and much of the free troposphere. Although this initial warming of the land surface would only cause a few tenths of a kelvin change in global-mean temperature, the resulting increase in outgoing longwave radiation from the Planck response of the land and free troposphere could account for an LA adjustment of the order of  $-1 \text{ W m}^{-2}$ . We would expect this adjustment process to be similar in most GCMs, so the differences in magnitude and sign of the LA forcing adjustment in Fig. 4 indicate that other forcing adjustment processes (probably involving water vapor) are present in other models (Andrews and Forster 2008).

The magnitude of the net forcing adjustment in the Hadley Centre models is increased beyond that due to LA through adjustment of the cloud. In HadGEM1, this is in the shortwave, while in HadCM3 it is in the longwave. SM00 and GW08 both show that the change in lapse rate resulting from the rapid warming of the troposphere compared to the ocean surface can cause a cloud change. To identify the types of cloud responsible for the adjustment, the change in each of the nine International Satellite Cloud Climatology Project (ISCCP) D2 cloud types (Rossow and Schiffer 1999) using model diagnostics from the ISCCP simulator (Klein and Jakob 1999; Webb et al. 2001; <http://gcss-dime.giss.nasa.gov/simulator.html>) has been regressed against  $T'$  for the two Hadley Centre models (HadGEM1 is shown in Fig. 6). In HadGEM1, regressions for most of the cloud types pass close to the origin, implying little forcing adjustment on time scales shorter than the stabilization period. However for low-top medium optical thickness cloud there is a considerable offset. This indicates a rapid increase in the amount of the cloud type during the period of ramped  $\text{CO}_2$  increase and results in the negative adjustment of SC. Medium thickness low cloud is often considered to be largely composed of stratocumulus. The initial increase in HadGEM1 is found to mainly occur over the stratocumulus/transition (to trade cumulus) regions on the eastern side of the subtropical ocean basins, and over the midlatitude oceans (particularly the Southern Ocean). Stratocumulus in these regions is capped by a strong inversion, hence the warming of the free troposphere relative to the surface and boundary layer implies the vertical temperature profile will become more stable; that is, the

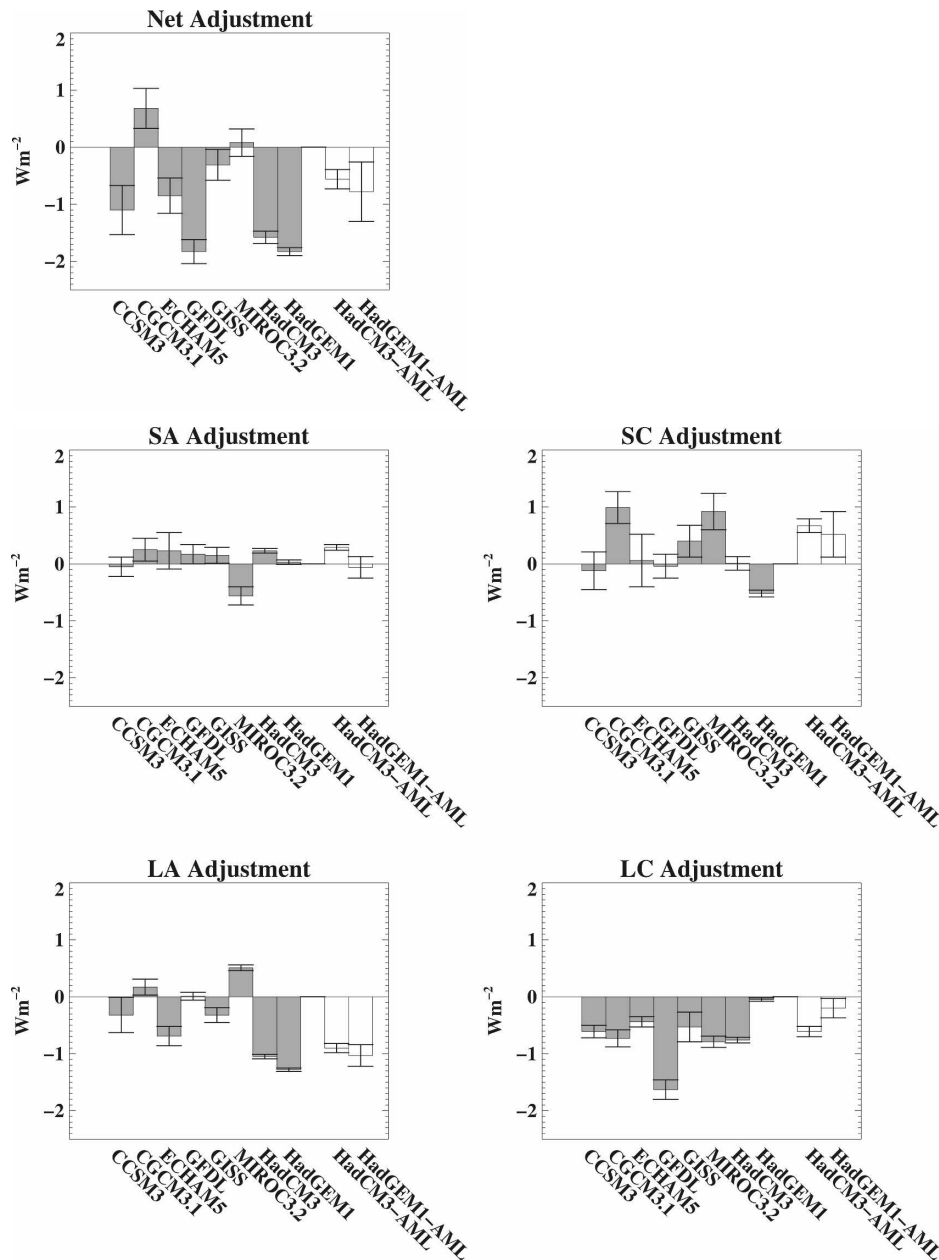


FIG. 4. Comparison of  $f_{\text{eff}}$  minus  $f_{\text{strat}}$  (i.e., the forcing adjustment) and its component parts. Results for each CMIP AO model are shown together with the AML versions of HadCM3 and HadGEM1. Uncertainties are  $\pm 1$  standard error from the regression; no error has been assumed for  $f_{\text{strat}}$ . Autocorrelation has not been accounted for in these uncertainty estimates.

strength of the inversion will increase. Williams et al. (2006) show that low cloud in many models is sensitive to the local saturated stability profile, with low cloud increasing when the profile is more stable owing to the presence of a stronger inversion. Over the regions where there is an initial increase in low cloud, there is also an increase in saturated stability at the initial time of  $\text{CO}_2$  doubling (illustrated for one region in Table 4).

During the stabilization period of the AO simulation, the inversion strength remains constant or weakens as the surface warms, and other processes (possibly circulation changes and/or changes to the boundary layer humidity structure) contribute to reduce the amount of this cloud type in some locations, at a rate that is roughly proportional to the surface temperature increase. In regions where there is no inversion and, so,

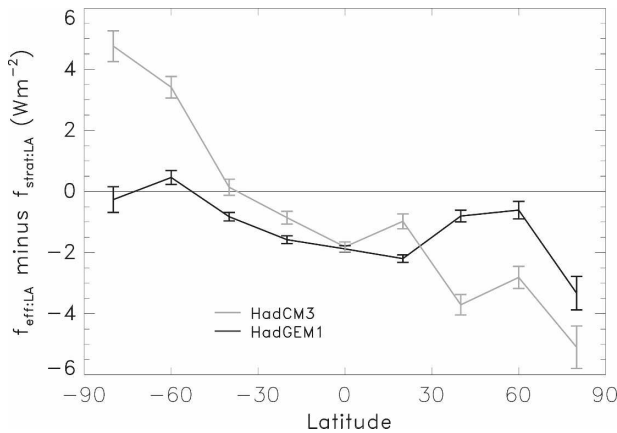


FIG. 5. Zonal-mean difference between the LA component of  $f_{\text{eff}}$  and  $f_{\text{strat}}$  for HadCM3 and HadGEM1. The plot is constructed from averages over  $20^\circ$  latitude bands (regressions over smaller regions tend to have poor signal to noise);  $f_{\text{eff,LA}}$  is obtained from the linear regression of the mean  $R'_{\text{LA}}$  in each latitude band against global-mean  $T'$  using decadal means for the AO model during stabilization. Error bars are  $\pm 1$  standard error from the regressions. Autocorrelation has not been accounted for in these uncertainty estimates.

more coupling between the boundary layer and free troposphere (e.g., over deep convective regions), the stability of the profile responds more linearly to global-mean warming in HadGEM1 (Table 4); hence there is little adjustment of other cloud types.

In HadCM3, there is a similar low cloud adjustment affecting the same regions as HadGEM1, but also an initial reduction in high cloud along the oceanic inter-tropical convergence zone and over the midlatitude oceans (not shown). Similar to the mechanism found by SM00 for HadCM2, this suggests that the initial increase in stability reduces the amount of deep convective cloud and convectively generated cirrus, providing a negative forcing adjustment of LC and a positive forcing adjustment of SC. The latter cancels the negative SC climate adjustment due to the increase in low cloud; hence for HadCM3 the longwave cloud adjustment dominates in the global mean. All of the CMIP3 models except HadGEM1 have a reasonably large negative global-mean LC forcing adjustment, suggesting that the initial convective cloud adjustment identified by SM00 may be common in GCMs.

### b. Time scale of the forcing adjustment

The results from the CMIP3 models are based on linear regressions through the stabilization period. On the basis of these experiments, we can only conclude that the forcing adjustment occurs sometime during the 70-yr ramped increase in  $\text{CO}_2$ . GW08 show that most of

the forcing adjustment in the AML models is within the first year; however, the magnitude of the AO forcing adjustments differ from the AML forcing adjustments, so the processes involved and their time scales may also differ. We investigate the time scale of the forcing adjustment in an AO model using a HadCM3 experiment in which  $\text{CO}_2$  is instantaneously doubled, rather than a ramped increase. Beyond the first two to three decades of this simulation, the linear relationship between  $R'$  and  $T'$  follows that of the stabilization following the ramped increase (Fig. 7a). However, during the first couple of decades following the instantaneous doubling of  $\text{CO}_2$ ,  $\Lambda$  is greater (i.e., the gradient of Fig. 7a is steeper and  $T'_{\text{eff}}$  is smaller) than later in the stabilization period. This indicates that the time scale of the forcing adjustment in HadCM3 is around two to three decades. This forcing adjustment time scale is consistent with an instantaneous  $4 \times \text{CO}_2$  simulation of HadCM3 (shown in Gregory et al. 2004 as experiment 4S) that also reveals a larger  $\Lambda$  for the first three decades before the data falls within a long stabilization simulation with a lower  $\Lambda$ . The comparison of the 2 and 4 ( $\times \text{CO}_2$ ) experiments suggests that the two to three decade time scale for the forcing adjustment is reasonably independent of the global  $T'$ .

Most of the LA forcing adjustment is found to occur within the first year, consistent with the establishment of an initial land–sea contrast on this time scale (Fig. 7b) and with a similar LA forcing adjustment being present in the AML models within the first year. Beyond this, the land–sea contrast reduces slightly, and reasonably linearly, with temperature as the ocean warms. There is some indication that the land–sea contrast is slightly higher for the first two decades (although this is not statistically significantly different from the linear regression), contributing to a small part of the decadal time-scale forcing adjustment. Much of the initial reduction in convective cloud in HadCM3 is also found to occur within the first year, again consistent with the AML results of GW08. Since the boundary layer is closely coupled to the free troposphere in deep convective regions, the amount of deep convective cloud quickly starts to increase (following the initial reduction) as the boundary layer warms.

Most of the decadal time-scale forcing adjustment is due to SC. The change in ocean surface temperature in some regions, particularly the eastern side of tropical ocean basins and parts of the Southern Ocean, remains small for the first few decades of the AO simulation. These are the same regions as identified previously for the low-cloud SC adjustment. The delayed ocean surface temperature response is illustrated for a region of the tropical southeast Pacific in Fig. 7c, which may be

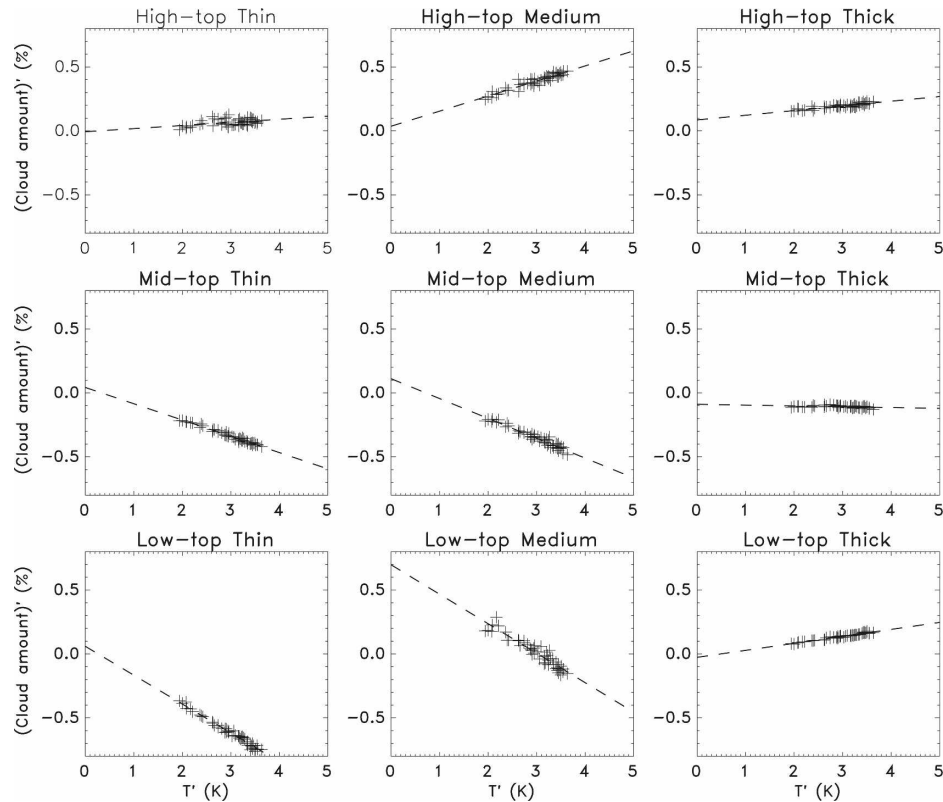


FIG. 6. HadGEM1: Global decadal-mean change in each of the ISCCP D2 cloud types from the ISCCP simulator plotted against the change in surface temperature ( $T'$ ) for the  $2 \times \text{CO}_2$  AO stabilization. Dashed lines show a linear regression through the data.

regarded as a transition region between stratocumulus and trade cumulus. Although the global-mean temperature increase for the second decade of the simulation with instantaneous  $\text{CO}_2$  doubling is 1.9 K, the local temperature in this region has only increased by 0.3 K. Since the free troposphere warms reasonably homogeneously, the local inversion strength increases during the first couple of decades, resulting in an increase in low cloud and associated strengthening of the local SCRE (Fig. 7d). Beyond the first few decades, SCRE' either remains fairly constant (as in Fig. 7d for the

tropical southeast Pacific) or starts to reduce as the surface warms. The AML models have a uniform mixed layer depth and do not have a dynamic ocean. Consequently, these regions do not remain anomalously cool on decadal time scales in the AML version and, as a result, there are significant differences between the SC forcing adjustment in the AO and AML models (Fig. 4). Although some of the initial increase in low cloud may be expected to diminish during stabilization, further feedbacks resulting from the presence of the cloud early in the simulation may contribute to  $T'_{\text{eq}}$  not being the same in the AO and AML models.

TABLE 4. Difference in equivalent saturated potential temperature ( $\theta_{\text{es}}$ ) between 700 and 1000 hPa (K) for the HadGEM1 control, at the initial time of  $\text{CO}_2$  doubling following the ramped  $\text{CO}_2$  increase, and after 500-yr stabilization (20-yr averages are used in the latter two cases). Results are shown for a stratocumulus region in the North Atlantic ( $20^\circ\text{--}40^\circ\text{N}$ ,  $10^\circ\text{--}30^\circ\text{W}$ ) and a deep convective region over the Pacific warm pool ( $10^\circ\text{S--}10^\circ\text{N}$ ,  $130^\circ\text{--}150^\circ\text{E}$ ).

Region	Control	At $2 \times \text{CO}_2$	After 500-yr stabilization
Stratocumulus	2.6	6.3	5.3
Deep convective	-17.7	-19.3	-20.3

## 6. Conclusions and discussion

In a comparison of CMIP3 models undergoing stabilization to doubling  $\text{CO}_2$ , the use of stratospherically adjusted forcings can be considered to produce a spurious centennial time evolution of effective climate sensitivity. Regression of  $R'$  against  $T'$  suggests that the feedback components are approximately constant for all of the GCMs, indicating little time/state dependence on these centennial time scales. The use of climate sen-

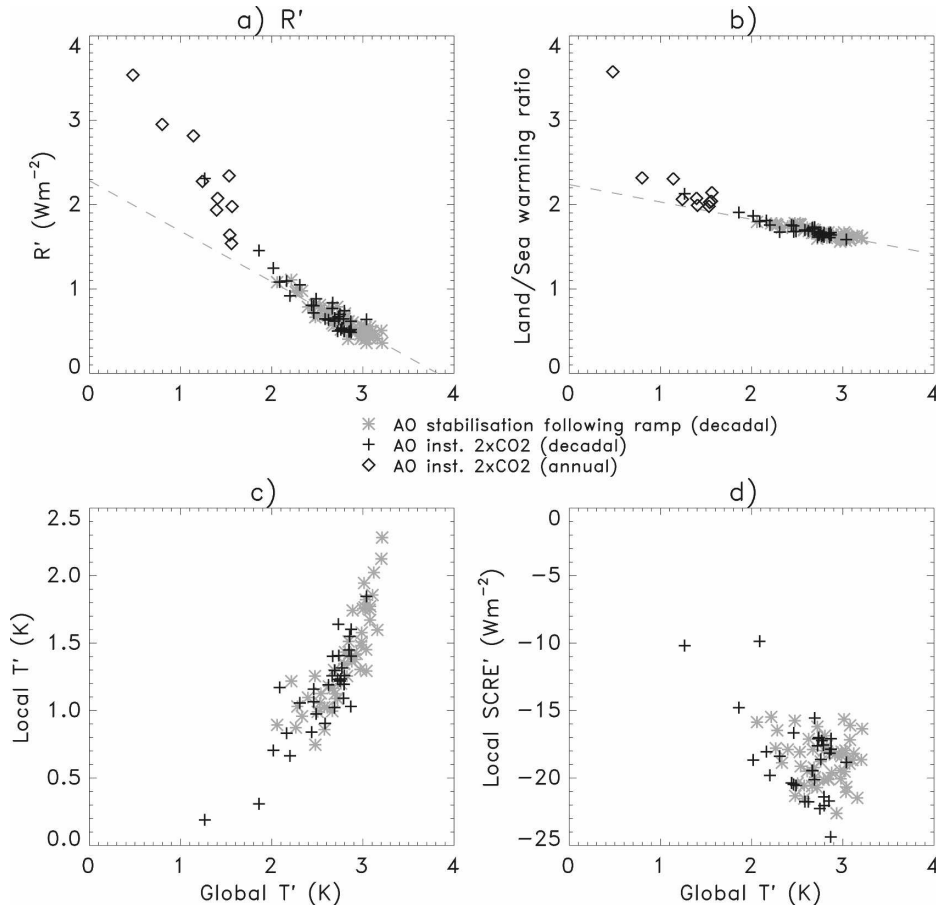


FIG. 7. HadCM3: (a) Global mean  $R'$ ; (b) ratio between global-mean land and sea surface temperature change; (c) temperature change over the region  $5^{\circ}\text{--}15^{\circ}\text{S}$ ,  $100^{\circ}\text{--}130^{\circ}\text{W}$ ; (d) change in SCRE over the same region. All are plotted against the global-mean temperature change. Gray data points are decadal means for the AO model during stabilization at  $2\times\text{CO}_2$  following the ramped increase in  $\text{CO}_2$  [in the case of (a), these are the same data as plotted in Fig. 1a]. The dashed lines [(a), (b)] are a linear regression through these data. Black crosses are decadal means from the AO model with instantaneous  $\text{CO}_2$  doubling. The black diamonds are the first 10 annual means from the AO model with instantaneous  $\text{CO}_2$  doubling [these are not shown for (c) and (d) since the signal is small compared to the noise].

sitivity assumes approximate proportionality between forcing and temperature response. The lack of any evolution of effective climate sensitivity during the stabilization period indicates that this assumption is valid for stabilization situations, provided that an effective forcing is used that is adjusted to account for processes acting on time scales shorter than the period under study. This is most easily achieved by using linear regression to obtain  $R'$  in the limit as  $T'$  tends to 0.

The difference between  $f_{\text{strat}}$  and  $f_{\text{eff}}$  represents adjustment of the climate system (other than in the stratosphere) on time scales that are rapid compared with those of global climate change. Part of this adjustment is likely to be due to the rapid warming of the land surface and free troposphere relative to the ocean sur-

face. However, the forcing adjustment is complicated by other processes such as cloud responses to the local change in lapse rate and changes to the distribution of water vapor. As a result, there is little agreement on the sign or magnitude of the net forcing adjustment. In the case of the Met Office Hadley Centre models, the largest contribution is from the warming of the land surface with a secondary contribution from an increase in low cloud, both acting to reduce the adjusted forcing. In the case of HadCM3, there is also a reduction of deep convective cloud and cirrus. There is some indication that a similar convective cloud adjustment may occur in many of the GCMs.

In several GCMs, the feedback parameter,  $\Lambda$ , and its components are found to differ between the AO ver-

sion undergoing stabilization and the AML version at equilibrium. While it is possible that there are future temperature thresholds for some of the feedbacks in the AO models, it is unlikely that they will all closely converge on the AML values. This difference between the AO and AML feedbacks occurs whether the stratospherically adjusted forcing or that obtained from regression is used. While AML models can still be useful as part of a hierarchy of simpler models to AOGCMs for understanding and comparing mechanisms within the atmospheric response, it seems that they can only quantitatively predict the equilibrium sensitivity of their AO counterparts to within about 0.5 K (the root-mean-square difference between the AO effective and AML equilibrium climate sensitivities of the models investigated).

The magnitude and time scale of the forcing adjustment appears to differ between the AO and AML models. Investigations with HadCM3 reveal that the forcing adjustment of the AO model can take a couple of decades following an instantaneous increase in  $\text{CO}_2$ , whereas in the AML model the forcing adjustment is within the first year. The two to three decade forcing adjustment in the AO model is due to parts of the ocean surface warming little on this time scale, resulting in a reduced lapse rate and increase in low cloud.

It has previously been suggested that fixed (sea) surface temperature experiments could be used to determine the adjusted forcing. However, owing to the dependence of the forcing adjustment on the evolution of the ocean, the resulting adjusted forcing may still be inappropriate for stabilization of the coupled climate system. AO experiments in which  $\text{CO}_2$  (or another forcing agent) is instantaneously changed and run for several decades toward equilibrium may be the most appropriate method for determining the effective forcing through the regression method. Such an experiment may also be used to further investigate the time scale and mechanisms of the forcing adjustment, and, if carried out as part of a coordinated project, would permit the differences in the magnitude and sign of the forcing adjustment between GCMs to be investigated.

The importance of responses acting on different time scales for simple energy balance models was noted by SM00. These models are often used to predict  $T'_{\text{eq}}$  of GCMs for different forcings. This study indicates that use of regressed  $f_{\text{eff}}$  and  $\Lambda$ , calculated through the experimental design proposed above, would improve the approximation of these simple models to the GCM.

Perhaps the most significant implication of having responses on different time scales is for the transient climate change response to changing forcing. The response to  $2 \times \text{CO}_2$  in Fig. 7a for HadCM3 can be ap-

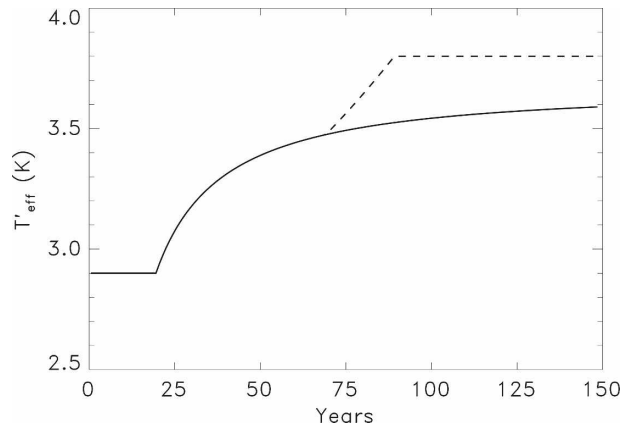


FIG. 8. Predicted evolution of  $2 \times \text{CO}_2$   $T'_{\text{eff}}$  in a HadCM3 simulation with  $\text{CO}_2$  increased at  $1\% \text{ yr}^{-1}$  throughout (solid) and with  $\text{CO}_2$  concentrations held fixed at  $2 \times \text{CO}_2$  after 70 yr (dashed), assuming independent responses to annual forcing increments. This is based on  $T'_{\text{eff}}$  obtained from Fig. 7a for the first 20 yr vs the remaining stabilization period.

proximated as  $T'_{\text{eff}}$  being 2.9 K for the first couple of decades following a change in forcing and thereafter being 3.8 K (obtained from the intercept of linear regression with the  $T'$  axis). If each forcing increment is assumed to lead to independent responses, then in a simulation of HadCM3 with  $\text{CO}_2$  increased at  $1\% \text{ yr}^{-1}$  the  $2 \times \text{CO}_2$  effective climate sensitivity will evolve as Fig. 8. It is not clear from Fig. 7a exactly how fast the change between the two climate sensitivities occurs, and the abrupt change at year 20 in Fig. 8 may be smoothed over a couple of decades. Of course,  $\text{CO}_2$  concentrations are currently increasing in the real world, so, on the basis of the GCM results presented here, the linear climate sensitivity concept may be inappropriate for considering climate change over the next few decades. Instead, it is probably more appropriate to consider responses acting on different time scales. For example, if the HadCM3 time scales are correct, there will be a climate adjustment occurring for the next couple of decades from current emissions, but there will also be longer time-scale feedbacks due to earlier forcings. As a result, it may be difficult to separate the responses occurring on different time scales observationally, and estimates of equilibrium climate sensitivity based on current climate change may be inaccurate.

In the situation when the external forcing agent is changing, Eq. (1) may be generalized to provide  $\Lambda$  at time  $t$  as

$$\Lambda = \frac{\left( R' - \int_{-\infty}^t G(t-t^*) \frac{df_{\infty}}{dt^*} dt^* \right)}{T'}, \quad (3)$$

where  $G$  is a response function equal to the ratio of the forcing effective after a finite time to the eventual value  $f_{\infty}$ . The integral gives the total forcing active at time  $t$  due to emissions (or other imposed changes) at all previous times  $t^*$ . In HadCM3, if the forcing agent becomes fixed, then  $G$  will become 1 after a couple of decades ( $t_{\text{adj}}$ ). If there are no subsequent variations in response, then the integral will remain constant, providing a useful separation of forcing and feedback for time scales beyond  $t_{\text{adj}}$ . Since the forcing adjustment will be relatively more important to the overall response when the forcing is changing than during a period of stabilization, understanding the differing climate adjustments among GCMs should be a priority for reducing uncertainty in model predictions of twenty-first-century climate change.

*Acknowledgments.* This work was supported by the Joint Defra and MoD Programme, (Defra) GA01101 (MoD) CBC/2B/0417\_Annex C5. We thank Mark Webb and Mark Ringer for their useful comments on the study. We acknowledge the modeling groups for making their simulations available for analysis, the Program for Climate Model Diagnosis and Intercomparison (PCMDI) for collecting and archiving the CMIP3 model output, and the WCRP's Working Group on Coupled Modelling (WGCM) for organising the model data analysis activity. The WCRP CMIP3 multimodel dataset is supported by the Office of Science, U.S. Department of Energy.

## REFERENCES

- Andrews, T., and P. M. Forster, 2008: CO<sub>2</sub> forcing induces semi-direct effects with consequences for climate feedback interpretations. *Geophys. Res. Lett.*, **35**, L04802, doi:10.1029/2007GL032273.
- Boer, G. J., and B. Yu, 2003a: Climate sensitivity and climate state. *Climate Dyn.*, **21**, 167–176.
- , and —, 2003b: Climate sensitivity and response. *Climate Dyn.*, **20**, 415–429.
- , and —, 2003c: Dynamical aspects of climate sensitivity. *Geophys. Res. Lett.*, **30**, 1135, doi:10.1029/2002GL016549.
- Cess, R. D., and Coauthors, 1990: Intercomparison and interpretation of climate feedback processes in 19 atmospheric general circulation models. *J. Geophys. Res.*, **95**, 16 601–16 615.
- Collins, W. D., and Coauthors, 2006: The Community Climate System Model version 3 (CCSM3). *J. Climate*, **19**, 2122–2143.
- Delworth, T. L., and Coauthors, 2006: GFDL's CM2 global coupled climate models. Part 1: Formulation and simulation characteristics. *J. Climate*, **19**, 643–674.
- Gordon, C., C. Cooper, C. A. Senior, H. Banks, J. M. Gregory, T. C. Johns, J. F. B. Mitchell, and R. A. Wood, 2000: The simulation of SST, sea ice extents and ocean heat transports in a version of the Hadley Centre coupled model without flux adjustments. *Climate Dyn.*, **16**, 147–168.
- Gregory, J. M., and M. J. Webb, 2008: Tropospheric adjustment induces a cloud component in CO<sub>2</sub> forcing. *J. Climate*, **21**, 58–71.
- , and Coauthors, 2004: A new method for diagnosing radiative forcing and climate sensitivity. *Geophys. Res. Lett.*, **31**, L03205, doi:10.1029/2003GL018747.
- Hansen, J., and Coauthors, 2002: Climate forcings in Goddard Institute for Space Studies SI2000 simulations. *J. Geophys. Res.*, **107**, 4347, doi:10.1029/2001JD001143.
- Houghton, J. T., Y. Ding, D. J. Griggs, M. Noguer, P. J. van der Linden, X. Dai, K. Maskell, and C. A. Johnson, Eds., 2001: *Climate Change 2001: The Scientific Basis*. Cambridge University Press, 881 pp.
- Johns, T. C., R. E. Carnell, J. F. Crossley, J. M. Gregory, J. F. B. Mitchell, C. A. Senior, S. F. B. Tett, and R. A. Wood, 1997: The second Hadley Centre coupled ocean–atmosphere GCM: Model description, spinup and validation. *Climate Dyn.*, **13**, 103–134.
- , and Coauthors, 2006: The new Hadley Centre climate model HadGEM1: Evaluation of coupled simulations. *J. Climate*, **19**, 1327–1353.
- K-1 Model Developers, 2004: K-1 coupled GCM (MIROC) description. K-1 Tech. Rep. 1, Center for Climate System Research, University of Tokyo, 39 pp.
- Kiehl, J. T., C. A. Shields, J. J. Hack, and W. D. Collins, 2006: The climate sensitivity of the Community Climate System Model version 3 (CCSM3). *J. Climate*, **19**, 2584–2596.
- Klein, S. A., and C. Jakob, 1999: Validation and sensitivities of frontal clouds simulated by the ECMWF model. *Mon. Wea. Rev.*, **127**, 2514–2531.
- Lambert, F. H., and N. E. Faull, 2007: Tropospheric adjustment: The response of two general circulation models to a change in insolation. *Geophys. Res. Lett.*, **34**, L03701, doi:10.1029/2006GL028124.
- Martin, G. M., M. A. Ringer, V. D. Pope, A. Jones, C. Dearden, and T. J. Hinton, 2006: The physical properties of the atmosphere in the new Hadley Centre Global Environmental Model (HadGEM1). Part I: Model description and global climatology. *J. Climate*, **19**, 1274–1301.
- Murphy, J. M., 1995: Transient response of the Hadley Centre coupled ocean–atmosphere model to increasing carbon dioxide. Part III: Analysis of global-mean response using simple models. *J. Climate*, **8**, 496–514.
- , D. M. H. Sexton, D. N. Barnett, G. S. Jones, M. J. Webb, M. Collins, and D. A. Stainforth, 2004: Quantification of modelling uncertainties in a large ensemble of climate change simulations. *Nature*, **430**, 768–772.
- Pope, V. D., M. L. Gallani, P. R. Rowntree, and R. A. Stratton, 2000: The impact of new physical parametrizations in the Hadley Centre climate model: HadAM3. *Climate Dyn.*, **16**, 123–146.
- Randall, D. A., and Coauthors, 2007: Climate models and their evaluation. *Climate Change 2007: The Physical Science Basis*, Solomon et al., Eds., Cambridge University Press, 589–662.
- Roeckner, E., and Coauthors, 2003: The atmospheric general circulation model ECHAM 5. Part I: Model description. Tech. Rep. 349, Max Planck Institute for Meteorology, 127 pp.
- Rossow, W. B., and R. A. Schiffer, 1999: Advances in understanding clouds from ISCCP. *Bull. Amer. Meteor. Soc.*, **80**, 2261–2287.
- Schmidt, G. A., and Coauthors, 2006: Present-day atmospheric simulations using GISS ModelE: Comparison to in situ, satellite, and reanalysis data. *J. Climate*, **19**, 153–192.

- Senior, C. A., and J. F. B. Mitchell, 2000: The time-dependence of climate sensitivity. *Geophys. Res. Lett.*, **27**, 2685–2688.
- Shine, K. P., J. Cook, E. J. Highwood, and M. M. Joshi, 2003: An alternative to radiative forcing for estimating the relative importance of climate change mechanisms. *Geophys. Res. Lett.*, **30**, 2047, doi:10.1029/2003GL018141.
- Soden, B. J., A. J. Broccoli, and R. S. Hemler, 2004: On the use of cloud forcing to estimate cloud feedback. *J. Climate*, **17**, 3661–3665.
- , I. M. Held, R. Colman, K. M. Shell, J. T. Kiehl, and C. A. Shields, 2008: Quantifying climate feedbacks using radiative kernels. *J. Climate*, **21**, 3504–3520.
- Stainforth, D. A., and Coauthors, 2005: Uncertainty in predictions of the climate response to rising levels of greenhouse gases. *Nature*, **433**, 403–406.
- Webb, M., C. A. Senior, S. Bony, and J.-J. Morcrette, 2001: Combining ERBE and ISCCP data to assess clouds in the Hadley Centre, ECMWF and LMD atmospheric climate models. *Climate Dyn.*, **17**, 905–922.
- Williams, K. D., A. Jones, D. L. Roberts, C. A. Senior, and M. J. Woodage, 2001a: The response of the climate system to the indirect effects of anthropogenic sulfate aerosol. *Climate Dyn.*, **17**, 845–856.
- , C. A. Senior, and J. F. B. Mitchell, 2001b: Transient climate change in the Hadley Centre models: The role of physical processes. *J. Climate*, **14**, 2659–2674.
- , and Coauthors, 2006: Evaluation of a component of the cloud response to climate change in an intercomparison of climate models. *Climate Dyn.*, **26**, 145–165, doi:10.1007/s00382-005-0067-7.
- Zhang, M. H., R. D. Cess, J. J. Hack, and J. T. Kiehl, 1994: Diagnostic study of climate feedback processes in atmospheric general circulation models. *J. Geophys. Res.*, **99**, 5525–5537.